The IRM Quarterly
Winter 2009/2010, Vol. 19 No. 4
ISSN: 2152-1972

Inside...

New Low-Temp Probe for 3-Axis Magnetic Measurements

Julie Bowles, Peter Solheid, Mike Jackson, Joshua Feinberg, and Bruce Moskowitz
IRM

The magnetic properties of geologic materials offer insights into an enormous range of important geophysical phenomena ranging from core dynamics to paleoclimate. Often it is the low-temperature behavior (<300 K) of magnetic minerals that provides the most useful and highest sensitivity information for a given problem. A material's low temperature magnetic behavior can indicate the dominant magnetic mineral phases, determine the grain size distribution of the constituent magnetic minerals, and even reveal evidence of biogenic iron minerals. Low-temperature cycling across the magnetite Verwey transition is sometimes used to remove remanence associated with multi-domain grains, which is undesirable for paleointensity and other paleomagnetic experiments. (Many of these low-temperature phenomena will be addressed in upcoming installments of our ongoing series on interpretation of low-temperature magnetic data.)

Despite the utility of low-temperature magnetic data, probing these low-temperature phenomena from the perspective of understanding the underlying physical behavior has been hampered by instrumental limitations. Until now, nearly all measurements of low-temperature magnetization have been single-axis and are rarely done in true zero-field environments. Low-temperature remanence measurements at the IRM have been carried out almost exclusively on the Quantum Designs Magnetic Properties Measurement System (MPMS) where magnetization is measured only in the vertical direction, and "zero-fields" of up to 1 μT are common. If low-temperature measurements of a natural remanence (NRM) are desired, great care must be taken to align the NRM with the measurement axis, and any directional change during thermal cycling will not be captured.

The IRM – with funding from the Instrumentation and Facilities Program of the National Science Foundation, Earth Science Division, and in conjunction with ColdEdge Technologies (Allentown, Pennsylvania) – has now developed a low-cost, cryogenic insert designed to work with a standard, horizontal-loading, 2G Enterprises magnetometer. Full three-axis measurements may now be made in ultra-low-field environments (nT) and under controlled heating and cooling from ~17 K to room temperature. The design is compatible with both the large (7.6 cm) and small (4.2 cm) bore magnetometers, as well as many standard pulse magnetizers. Used in conjunction with the in-line degausser on the IRM's pass-through magnetometer, it will ultimately be possible to acquire anhysteretic remanence (ARM) and/or AF demagnetize samples at cryogenic temperatures.

Figure 1. Peter Solheid makes an adjustment to the low-temperature probe.

Instrument Design

The cryogenic insert is cooled by a pneumatically-driven Displex SHI SH-204 10K two-stage cryocooler with a 73.7 cm copper cold tip extension and 3.8 cm diameter stainless steel vacuum shroud (Fig. 2). A 40.6 cm sapphire cold tip extension and sapphire radiation shield are joined to the end of the copper extension in order to prevent any disturbance to the measurement region of the magnetometer. A fiberglass vacuum shroud extension mounts to the stainless shroud to provide a non-metallic extension to the vacuum insulation space. Temperature control is provided by a non-inductively wound, 50 watt heater integrated into the body of the probe and mounted out of the sensor region 40.6 cm away from the sample. The temperature inside the probe is monitored directly at

cont'd. on pg. 6...

8th Santa Fe Conference on Rock Magnetism to be held June 24 - 27

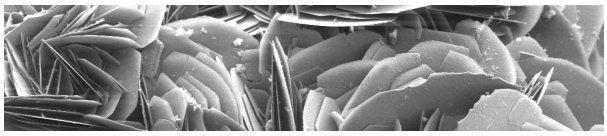

The Eighth Santa Fe Conference on Rock Magnetism will be held June 24 - 27 at St. John's College in Santa Fe, New Mexico. This small, intimate meeting has proven very popular, as the format allows for in-depth discussion of current topics in rock magnetism. Students are particularly encouraged to attend, and generous support by the **National Science Foundation** means that registration and housing fees will be waived for all participants. Additional funding is provided by **ASC Scientific**, **Bartington Instruments**, **Quantum Design**, and **Princeton Measurements Corporation**.

Program

The format of the conference involves one or two invited speakers in each session, followed by an extended period of open mic and discussion.

Wednesday, June 23

2:30 Check-in/registration begins for those arriving early for field trip

Thursday, June 24

8:30 Field trip departure to Valles Caldera

2:30 Check-in/registration begins for non-field trip participants

7:00 Welcome and Opening Comments
(Bruce Moskowitz, IRM, University of Minnesota)

7:10 Key-note lecture on dynamos and planetary magnetism
(Peter Olson, Johns Hopkins University)

Friday, June 25

9:00 Successful Developments in Paleointensity
(Coordinators: Joshua Feinberg & Yohan Guyodo)

1:30 Extra-terrestrial Magnetism: Materials and Processes
(Coordinators: Mike Fuller & Kristin Lawrence)

Evening Free

Saturday, June 26

9:00 Keynote lecture on Iron Chemistry, Mineralogy and Analytical Techniques
(Brandy Toner, Dept. of Soil, Water, and Climate, University of Minnesota)

10:45 Environmental Magnetism
(Coordinators: Christoph Geiss & Rich Reynolds)

2:00 Quantitative Modeling of Mineral Magnetic Data
(Coordinators: Andrew Newell & Aleksey Smirnov)

Evening Free

Sunday, June 27

7:30 Continental breakfast, Junior Commons

9:00 Teaching Paleomagnetism
(Coordinators: Bruce Moskowitz & Laurie Brown)

Optional Field Trip

An optional field trip to Valles Caldera will take place on the first day of the meeting from approximately 8:30 a.m. to 3:30 p.m. The rhyolitic domes of Valles Caldera – sampled near Jaramillo Creek – were used by Doell and Dalrymple (1966) to document the termination of a newly-discovered polarity subchron: the Jaramillo event. This work helped lead to the widespread acceptance of the Vine-Matthews-Morley hypothesis of seafloor spreading, by establishing a magnetic polarity timescale consistent with the marine magnetic anomaly observations. Although subsequent work has shown that the lavas actually record a later event (Singer and Brown, 2002), Valles Caldera is still where it all began.

The field trip will be led by John Geissman (University of New Mexico). A $110 fee will cover field trip expenses, including the extra night's lodging, meals, and transportation.

Registration Information

There will be no conference registration fee. Dormitory accommodations and meals in the St. John's cafeteria are provided by funding from the **National Science Foundation**. Travel expenses are the responsibility of individual participants.

A non-participating spouse or other guest will be charged $205 to cover three nights lodging, all meals and coffee breaks. A $110 fee will cover field trip expenses for those who choose to participate.

Visit the conference web site (**www.irm.umn.edu/SantaFe8/**) for registration form and additional information. **Registration closes May 31 or when available spaces are full.**

Cerro la Jara, a rhyolite dome within Valles Caldera. Valles Caldera National Preserve is the location of the field trip prior to the Santa Fe Meeting. (Photo from Wikipedia Commons)

Visiting Fellow's Reports

Magnetic properties of single crystals of ilmenite-hematite with magnetite from the Ecstall pluton, British Columbia

Sarah Brownlee
University of California, Berkeley
sbrownlee@berkeley.edu

The (~91 Ma) Ecstall pluton in northwest British Columbia has a complicated thermal history whereby it has been reheated by the younger (~58 Ma) Quottoon plutonic complex on its eastern margin [1]. The reheating caused changes in T-fO_2 conditions leading to mineralogic changes within the Fe-Ti oxides. At locations closer than ~14 km from the Quottoon plutonic complex the hematite in ilmenite-hematite is reducing to magnetite, and forming 20-50 nm sized magnetite crystals within the hematite [2]. There are corresponding changes in bulk magnetic properties across the Ecstall pluton; however, to confirm that changes in bulk magnetic properties are due to mineralogic changes within ilmenite-hematite grains, it is necessary to study the magnetic properties of single crystals.

Single crystals of ilmenite-hematite (~425-650 µm) were separated from crushed samples from 7 locations at varying distances from the Quottoon plutonic complex, herein referred to as the thermal boundary. We measured hysteresis properties using the alternating gradient magnetometer (AGM), remanence vs. temperature using the magnetic properties measurement system (MPMS), and isothermal remanence magnetization (IRM) acquisition using an impulse magnetometer.

Single crystal magnetic properties grouped into 3 groups corresponding to distance from the thermal boundary and the presence or absence of classic rutile blitz texture. Group 1 consists of locations farthest from the thermal boundary (> 14 km); group 2 is locations < 14 km from the thermal boundary with no rutile blitz texture; and group 3 is locations < 14 km from the thermal boundary with rutile blitz texture. In general, rutile blitz texture was only seen in locations <8 km from the thermal boundary.

The distinction between the three groups is most clearly seen in the hysteresis measurements (Fig 1). Group 1 hysteresis loops are typical of hematite. They have coercivities of 150-250 mT and M_r/M_s ratios of 0.8-0.95 after slope correction. This group is farthest from the thermal boundary and thus represents magnetic properties that are not affected by reheating. Group 2 hysteresis loops are wasp-wasted to varying degrees due to variable amounts of magnetite. The resulting coercivities range from 10-275 mT and M_r/M_s ranges from 0.1-0.85. Group 3 has similar hysteresis loops to group 2 except coercivities for group

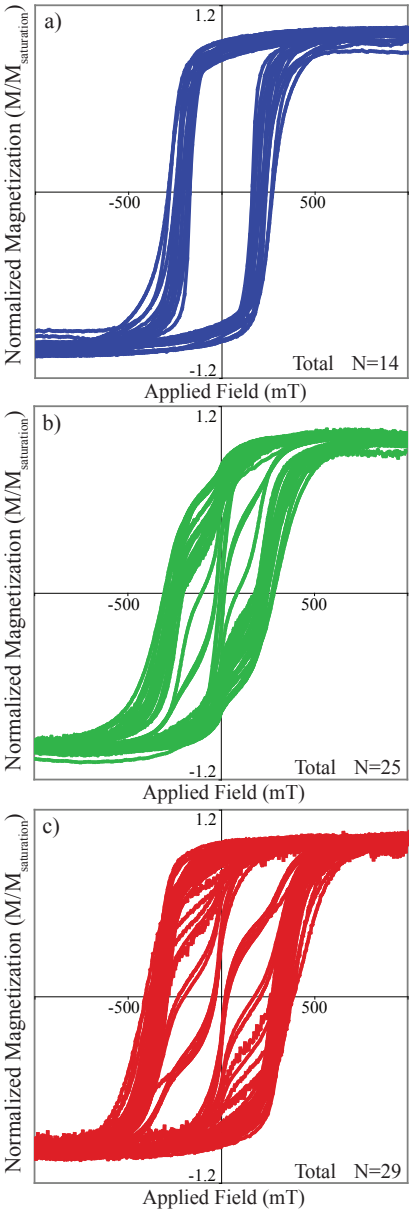

Figure 1. *Hysteresis loops from a) group 1, b) group 2, and c) group 3. Magnetization is normalized to the value at 1 T.*

3 are significantly higher, and range from ~10-400 mT.

The increase in coercivity from group 2 to group 3 has two potential explanations. The first is further exsolution of hematite and ilmenite lamellae during reheating above the miscibility gap. The second involves the rutile blitz texture itself. Blitz texture is made up of abundant rutile needles cutting through the ilmenite-hematite host in 6 different orientations, which could result in a reduction of magnetic domain size in hematite with a corresponding increase in coercivity. Also, the rutile needles themselves have exsolved hematite in them (Brownlee et al. 2010), which is likely to have high coercivity due to small size and high shape anisotropy.

The remanence vs. temperature, and IRM acquisition experiments complement the hysteresis measurements. In summary, grains from group 1 consist of only hematite and ilmenite. Grains from group 2 consist of hematite and ilmenite with varying amounts of magnetite resulting from reduction of hematite. Group 2 also tends to have more ilmenite than group 1, which is evident in the low

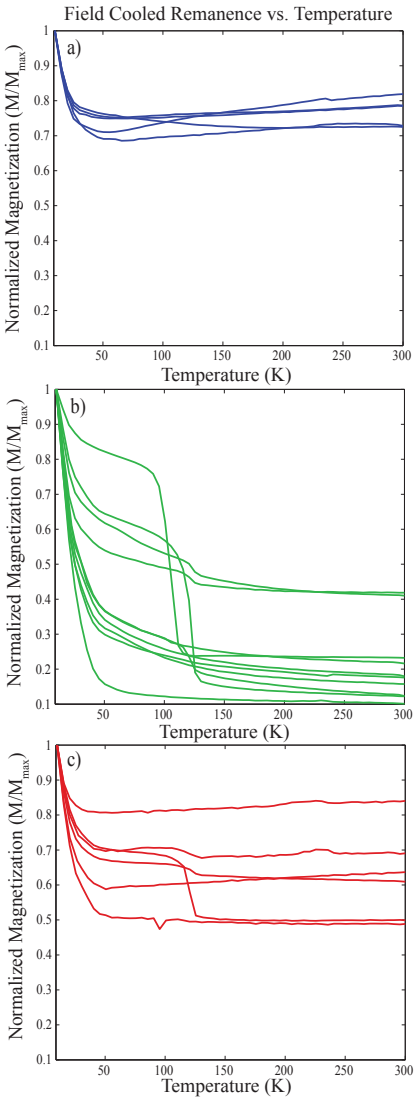

Figure 2. *Field cooled remanence vs. temperature curves for a) group 1, b) group 2, and c) group 3. The remanence magnetization is normalized to the maximum measured for each grain, which occurs at ~10 K. Presence of magnetite is indicated by clear Verway transitions at ~110-120 K in groups 2 and 3. Grains that contain a lot of ilmenite, which acquires remanence below ~40 K, are characterized by low values of M/Mmax at room temperature, i.e. group 2.*

temperature remanence curves (Fig. 2). Grains from group 3 are similar to group 2, but have higher coercivities.

These experiments have shown that changes in bulk magnetic properties across the Ecstall pluton can be explained by the magnetic properties of single crystals of ilmenite-hematite, and that the magnetic properties have been affected by reheating and subsequent growth of magnetite ~33 Ma after emplacement of the Ecstall pluton. Therefore, paleomagnetic directions from <14 km from the Quottoon plutonic complex are not likely to record ambient field conditions at the time of emplacement of the Ecstall pluton.

Many thanks to Gary Scott, and everyone at the IRM, in particular: Julie Bowles, Mike Jackson, Peat Solheid, and Josh Feinberg.

References:

[1] Brownlee, S.J., and Renne, P.R., 2010, *GCA*, in press.
[2] Brownlee, S.J., Feinberg, J.M., Harrison, R.J., Kasama, T., Scott, G.R., and Renne, P.R., 2010, *Am. Min.*, 95, 153-160.

Current Articles

A list of current research articles dealing with various topics in the physics and chemistry of magnetism is a regular feature of the IRM Quarterly. Articles published in familiar geology and geophysics journals are included; special emphasis is given to current articles from physics, chemistry, and materials-science journals. Most abstracts are taken from INSPEC (© Institution of Electrical Engineers), Geophysical Abstracts in Press (© American Geophysical Union), and The Earth and Planetary Express (© Elsevier Science Publishers, B.V.), after which they are subjected to Procrustean culling for this newsletter. An extensive reference list of articles (primarily about rock magnetism, the physics and chemistry of magnetism, and some paleomagnetism) is continually updated at the IRM. This list, with more than 10,000 references, is available free of charge. Your contributions both to the list and to the Abstracts section of the IRM Quarterly are always welcome.

Anisotropy/Magnetic Fabrics

Canon-Tapia, E., and E. Herrero-Bervera, Sampling strategies and the anisotropy of magnetic susceptibility of dykes, *Tectonophys.*, 466, 3-17, 2009.

Han, Y.L., X.D. Tan, and K.P. Kodama, Can rock magnetic fabric reveal strain? Case studies of Early Triassic limestones from South China Block, *Chinese J. Geophys.-Chinese Ed.*, 52 (10), 2588-2594, 2009.

Hrouda, F., O. Krejci, M. Potfaj, Z. Stranik, Magnetic fabric and weak deformation in sandstones of accretionary prisms of the Flysch and Klippen Belts of the Western Carpathians: Mostly offscraping indicated, *Tectonophys*., 479, 254-270, 2009.

Mamtani, M.A., A. Sengupta, Anisotropy of magnetic susceptibility analysis of deformed kaolinite: implications for evaluating landslides, *Int. J. Earth Sci*., 98, 1721-1725, 2009.

Masquelin, H., T. Aifa, R. Muzio, E. Hallot, G. Veroslavsky, and L. Bonnevalle, The Cuaro Mesozoic doleritic dyke swarm, southern Parana basin, Uruguay: Examples of superimposed magnetic fabrics?, *C.R. Geosci.*, 341, 1003-1015, 2009.

Schmidt, V., A.M. Hirt, B. Leiss, L. Burlini, and J.M. Walter, Quantitative correlation of texture and magnetic anisotropy of compacted calcite-muscovite aggregates, *J. Struct. Geol.*, 31 (10), 1062-1073, 2009.

Zavada, P., K. Schulmann, O. Lexa, F. Hrouda, J. Haloda, and P. Tycova, The mechanism of flow and fabric development in mechanically anisotropic trachyte lava, *J. Struct. Geol*., 31 (11), 1295-1307, 2009.

Archeomagnetism

Gallet, Y., A. Genevey, M. Le Goff, N. Warme, J. Gran-Aymerich, and A. Lefevre, On the use of archeology in geomagnetism, and vice-versa: Recent developments in archeomagnetism, *C.R. Physique*, 10 (7), 630-648, 2009.

Korte, M., M. Mandea, and J. Matzka, A historical declination curve for Munich from different data sources, *Phys. Earth Planet. Int.*, 177 (3-4), 161-172, 2009.

Lanza, R., E. Zanella, and S. Saudino, Magnetic remanence of hematite-bearing murals, *Geophys. Res. Lett*., 36, 2009.

Bio(geo)magnetism

Holland, R.A., J.L. Kirschvink, T.G. Doak, and M. Wikelski, Bats Use Magnetite to Detect the Earth's Magnetic Field, *PLoS One*, 3 (2), 2008.

Bokkon, I., and V. Salari, Information storing by biomagnetites,

J. Biol. Phys., 36 (1), 109-120, 2010.
Lin, W., and Y.X. Pan, Temporal variation of magnetotactic bacterial communities in two freshwater sediment microcosms, *Fems Microbiology Letters*, 302 (1), 85-92, 2010.
Winklhofer, M., The Physics of Geomagnetic-Field Transduction in Animals, *Ieee Trans. Magn.*, 45 (12), 5259-5265, 2009.

Environmental Magnetism and Paleoclimate Proxies

Abrajevitch, A., R. Van der Voo, and D.K. Rea, Variations in relative abundances of goethite and hematite in Bengal Fan sediments: Climatic vs. diagenetic signals, *Mar. Geol.*, 267 (3-4), 191-206, 2009.
Haltia-Hovi, E., N. Nowaczyk, T. Saarinen, and B. Plessen, Magnetic properties and environmental changes recorded in Lake Lehmilampi (Finland) during the Holocene, *J. Paleolimnology*, 43 (1), 1-13, 2010.
Hao, Q.Z., F. Oldfield, J. Bloemendal, J. Torrent, and Z.T. Guo, The record of changing hematite and goethite accumulation over the past 22 Myr on the Chinese Loess Plateau from magnetic measurements and diffuse reflectance spectroscopy, *J. Geophys. Res.*, 114, 2009.
Hiemstra, T., J. Antelo, R. Rahnemaie, and W.H. van Riemsdijk, Nanoparticles in natural systems I: The effective reactive surface area of the natural oxide fraction in field samples, *Geochim. Cosmochim. Acta*, 74 (1), 41-58, 2010.
Hiemstra, T., J. Antelo, A.M.D. van Rotterdam, and W.H. van Riemsdijk, Nanoparticles in natural systems II: The natural oxide fraction at interaction with natural organic matter and phosphate, *Geochim. Cosmochim. Acta*, 74 (1), 59-69, 2010.
Kissel, C., C. Laj, T. Mulder, C. Wandres, and M. Cremer, The magnetic fraction: A tracer of deep water circulation in the North Atlantic, *Earth Planet. Sci. Lett.*, 288, 444-454, 2009.
Kopp, R.E., D. Schumann, T.D. Raub, D.S. Powars, L.V. Godfrey, N.L. Swanson-Hysell, A.C. Maloof, and H. Vali, An Appalachian Amazon? Magnetofossil evidence for the development of a tropical river-like system in the mid-Atlantic United States during the Paleocene-Eocene thermal maximum, *Paleoceanography*, 24, 2009.
Lee, Y.S., and K. Kodama, A possible link between the geomagnetic field and catastrophic climate at the Paleocene-Eocene thermal maximum, *Geology*, 37 (11), 1047-1050, 2009.

Extraterrestrial Magnetism

Funaki, M., V. Hoffmann, and N. Imae, Estimate of the magnetic field of Mars based on the magnetic characteristics of the Yamato 000593 nakhlite, *Meteorit. Planet. Sci.*, 44 (8), 1179-1191, 2009.
Thomas-Keprta, K.L., S.J. Clemett, D.S. McKay, E.K. Gibson, and S.J. Wentworth, Origins of magnetite nanocrystals in Martian meteorite ALH84001, *Geochim. Cosmochim. Acta*, 73 (21), 6631-6677, 2009.
Yu, Y., S.J. Doh, W. Kim, and K. Min, Ancient stable magnetism of the Richardton H5 chondrite, *Phys. Earth Planet. Int.*, 177, 12-18, 2009.

Magnetic Field Records and Paleointensity methods

Ben-Yosef, E., L. Tauxe, T.E. Levy, R. Shaar, H. Ron, and M. Najjar, Geomagnetic intensity spike recorded in high resolution slag deposit in Southern Jordan, *Earth Planet. Sci. Lett.*, 287 (3-4), 529-539, 2009.
Ferk, A., and R. Leonhardt, The Laschamp geomagnetic field excursion recorded in Icelandic lavas, *Phys. Earth Planet. Int.*, 177 (1-2), 19-30, 2009.
Herrero-Bervera, E., and J.P. Valet, Testing determinations of absolute paleointensity from the 1955 and 1960 Hawaiian flows, *Earth Planet. Sci. Lett.*, 287 (3-4), 420-433, 2009.
Linder, J., and R. Leonhardt, Paleomagnetic full vector record of four consecutive Mid Miocene geomagnetic reversals, *Phys. Earth Planet. Int.*, 177 (1-2), 88-101, 2009.
Tauxe, L., and K.P. Kodama, Paleosecular variation models for ancient times: Clues from Keweenawan lava flows, *Phys. Earth Planet. Int.*, 177 (1-2), 31-45, 2009.
Yang, X.Q., F. Heller, J. Yang, and Z.H. Su, Paleosecular variations since ~9000 yr BP as recorded by sediments from maar lake Shuangchiling, Hainan, South China, *Earth Planet. Sci. Lett.*, 288 (1-2), 1-9, 2009.

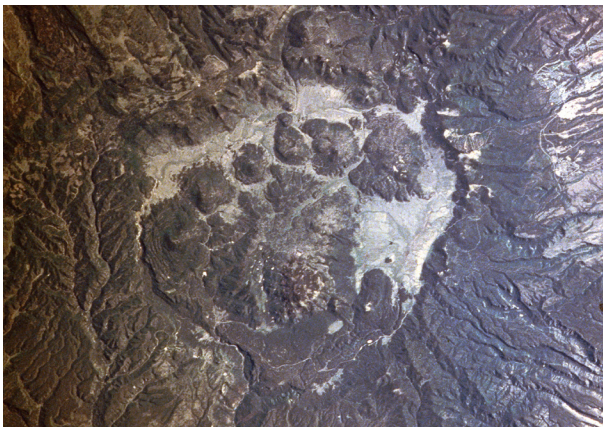

Valles Caldera (location of the field trip prior to the Santa Fe meeting) as seen from the Space Shuttle. Image courtesy of the Image Science & Analysis Laboratory, NASA Johnson Space Center. Image STS040-614-63, http://eol.jsc.nasa.gov/.

Rock and Mineral Magnetism

Brownlee, S.J., J.M. Feinberg, R.J. Harrison, T. Kasama, G.R. Scott, and P.R. Renne, Thermal modification of hematite-ilmenite intergrowths in the Ecstall pluton, British Columbia, Canada, *Am. Mineral.*, 95 (1), 153-160, 2010.
Gehring, A.U., H. Fischer, M. Louvel, K. Kunze, and P.G. Weidler, High temperature stability of natural maghemite: a magnetic and spectroscopic study, *Geophys. J. Int.*, 179 (3), 1361-1371, 2009.
Jacob, J., and M.A. Khadar, VSM and Mossbauer study of nanostructured hematite, *J. Magn. Magn. Mater.*, 322 (6), 614-621, 2010.
McCammon, C.A., S.A. McEnroe, P. Robinson, K. Fabian, and B.P. Burton, High efficiency of natural lamellar remanent magnetisation in single grains of ilmeno-hematite calculated using Mossbauer spectroscopy, *Earth Planet. Sci. Lett.*, 288 (1-2), 268-278, 2009.
Muxworthy, A.R., and W. Williams, Critical superparamagnetic/single-domain grain sizes in interacting magnetite particles: implications for magnetosome crystals, *J. R. Soc. Interface*, 6 (41), 1207-1212, 2009.
Newell, A., Transition to superparamagnetism in chains of magnetosome crystals, *Geochem. Geophys. Geosys.*, 10, 2009.
Oldfield, F., Q.Z. Hao, J. Bloemendal, Z. Gibbs-Eggar, S. Patil, and Z.T. Guo, Links between bulk sediment particle size and magnetic grain-size: general observations and implications for Chinese loess studies, *Sedimentology*, 56, 2091-2106, 2009.
Zhang, Z.J., L. Clime, B. Tomanek, G. Sutherland, and T. Veres, Low-temperature first-order reversal curves and interaction effects on assemblies of iron oxide nanoparticles, *Physica B-Condensed Matter*, 404 (20), 3666-3670, 2009.

Mineral Physics and Chemistry

Barbosa, P.F., and L. Lagoeiro, Crystallographic texture of the magnetite-hematite transformation: Evidence for topotactic relationships in natural samples from Quadrilatero Ferrifero, Brazil, *Am. Mineral.*, 95 (1), 118-125, 2010.

Blanchard, M., F. Poitrasson, M. Meheut, M. Lazzeri, F. Mauri, and E. Balan, Iron isotope fractionation between pyrite (FeS2), hematite (Fe_2O_3) and siderite ($FeCO_3$): A first-principles density functional theory study, *Geochim. Cosmochim. Acta*, 73, 6565-6578, 2009.

Bosch, J., K. Heister, T. Hofmann, and R.U. Meckenstock, Nano-sized Iron Oxide Colloids Strongly Enhance Microbial Iron Reduction, *Appl. Environ. Microbiol.*, 76, 184-189, 2010.

Martin, G.J., R.S. Cutting, D.J. Vaughan, and M.C. Warren, Bulk and key surface structures of hematite, magnetite, and goethite: A density functional theory study, *Am. Mineral.*, 94 (10), 1341-1350, 2009.

Pallud, C., M. Kausch, S. Fendorf, and C. Meile, Spatial Patterns and Modeling of Reductive Ferrihydrite Transformation Observed in Artificial Soil Aggregates, *Environ. Sci. Technol.*, 44 (1), 74-79, 2010.

Spalek, J., A. Kozlowski, Z. Kakol, Z. Tarnawski, Y. Fukami, F. Ono, R. Zach, L.J. Spalek, and J.M. Honig, Verwey transition in magnetite at high pressure: A new quantum critical point at the onset of metallization, *Physica B-Condensed Matter*, 404, 2894-2897, 2009.

Other

Klein, F., W. Bach, N. Jons, T. McCollom, B. Moskowitz, and T. Berquo, Iron partitioning and hydrogen generation during serpentinization of abyssal peridotites from 15 degrees N on the Mid-Atlantic Ridge, *Geochim. Cosmochim. Acta*, 73 (22), 6868-6893, 2009.

Maloof, A.C., S.T. Stewart, B.P. Weiss, S.A. Soule, N.L. Swanson-Hysell, K.L. Louzada, I. Garrick-Bethell, and P.M. Poussart, Geology of Lonar Crater, India, *Geol Soc. Am. Bull.*, 122 (1-2), 109-126, 2010.

McEnroe, S.A., L.L. Brown, and P. Robinson, Remanent and induced magnetic anomalies over a layered intrusion: Effects from crystal fractionation and magma recharge, *Tectonophys.*, 478 (1-2), 119-134, 2009.

Mitra, R., and L. Tauxe, Full vector model for magnetization in sediments, *Earth Planet. Sci. Lett.*, 286, 535-545, 2009.

Morris, A., J.S. Gee, N. Pressling, B.E. John, C.J. MacLeod, C.B. Grimes, and R.C. Searle, Footwall rotation in an oceanic core complex quantified using reoriented Integrated Ocean Drilling Program core samples, *Earth Planet. Sci. Lett.*, 287 (1-2), 217-228, 2009.

Tarduno, J.A., R.D. Cottrell, M.K. Watkeys, A. Hofmann, P.V. Doubrovine, E.E. Mamajek, D. Liu, D.G. Sibeck, L.P. Neukirch, Y. Usui, Geodynamo, Solar Wind, and Magnetopause 3.4 to 3.45 Billion Years Ago, *Science*, 327, 1238-1240, 2010.

IRM's new low-temp probe (continued from pg. 1)

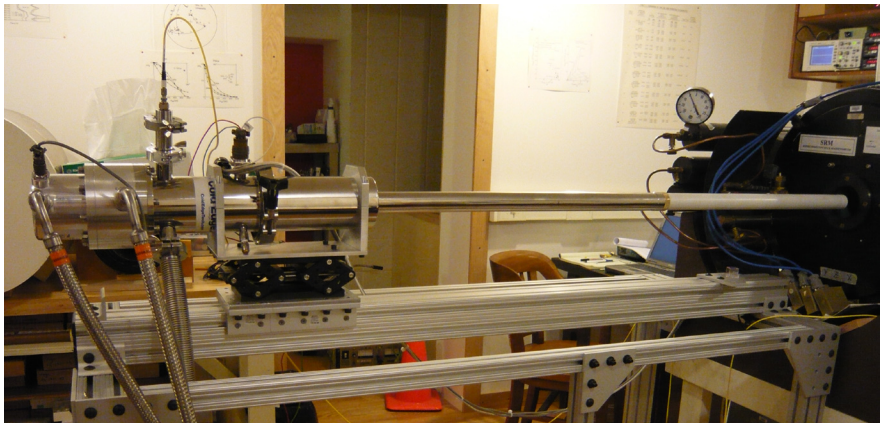

Figure 2. *Low-temperature insert installed on the IRM's RF SQUID magnetometer. On the left are the cryocooler and compressor lines. The fiberoptic temperature sensor extends vertically up from the cryocooler. On the right is the vacuum shroud extension.*

the sample using a non-magnetic, fiber-optic temperature sensor. Ultimately, the probe will be mounted on a translation table driven by a programmable stepper motor so that measurements may be automated.

Preliminary Results

The prototype instrument is still in the development and testing stage, but it is operational and early results are extremely encouraging. One of the many motivations for building the low-temperature probe was to better understand directional variations in magnetization across magnetic phase changes and isotropic points. For example, single-axis measurements on large, single-crystal magnetites have demonstrated that crystallographic orientation plays a large role in magnetization behavior across the Verwey transition (Özdemir and Dunlop, 1999).

As a test case, we selected a portion of a natural, single crystal magnetite octahedron that was roughly two millimeters across. A 1.2 T pulse field was applied at room temperature along either a [111] (easy) axis, a [110] (intermediate) axis, or a [100] (hard) axis. Following each treatment, the sample was cooled to ~20 K (requiring ~3 hrs) and then warmed back to room temperature (over another ~3 hrs) inside the probe. The sample was oriented so that a [100] axis was aligned with the magnetometer Z-axis (the long axis of the magnetometer and probe), while two <110> axes were aligned with magnetometer X and Y. During this initial testing only, sample orientation with respect to both the applied field and the measurement axes was approximate, and misorientations of up to ~10º are likely.

Results from the [111] case are shown in Figure 3. The room-temperature magnetization is somewhat shallower than would be expected if it were constrained by magnetocrystalline anisotropy to lie along [111]; however the possible sample misorientations may be contributing to this. Magnetization on cooling decreases across the

Verwey transition, reaching a minimum at ~115 K before rapidly increasing to ~50% of the room temperature remanence. The same pattern is observed on all three measurement axes. On warming, this behavior is completely reversible for T < 115 K, and there is no indication of any temperature lag or thermal hysteresis. Above this temperature the warming remanence is considerably less than the cooling remanence due to irreversible domain wall motions. Aside from a subtle clockwise rotation of the remanence on cooling, no directional change is discernible, as might be expected from a rotation of the remanence vector from the cubic [111] easy axis at T > T_V to the monoclinic [100] easy axis at T < T_V.

We note that some of the subtle directional variation may be due to an inadequate background correction; a silicon diode temperature sensor with relatively high magnetization (~ 10^{-6} Am^2) is currently mounted near the sample for calibration of the fiber optic temperature sensor. The diode magnetization varies in a roughly linear fashion with temperature, and the correction for this is imperfect. Temperature calibration is still being improved (there is a roughly 5 K constant temperature offset in the shown test data), and the diode will ultimately be removed.

When the field is applied along the [100] (hard) axis (Fig. 4), the magnetization lies mostly along that axis, but ~20% along one of the intermediate axes ([110], magnetometer Y). The second intermediate axis ([$\bar{1}$10], magnetometer X) is essentially zero at room temperature.

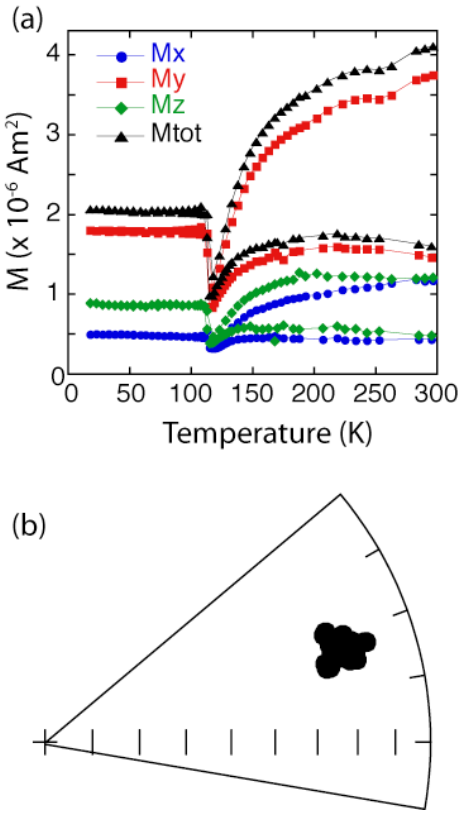

Figure 3. *Low-temperature cycling of a 1.2 T isothermal remanence applied along the sample [111] (easy) axis.* ***(a)*** *Magnetization vs. temperature in magnetometer coordinates (X, Y, Z, and total). M_Z is roughly along the [001] (hard) axis, while M_X and M_Y are along two of the intermediate axes: [$\bar{1}$10] and [110], respectively.* ***(b)*** *Equal-area diagram showing little directional change as the sample cools and warms.*

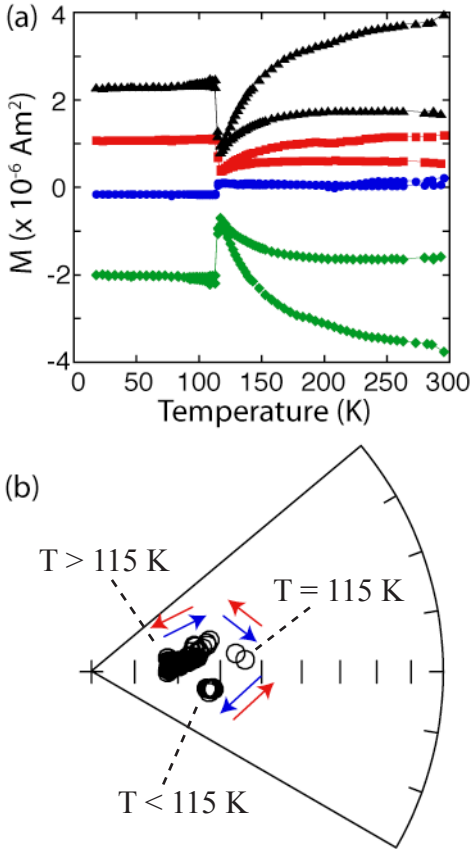

Figure 4. *Low-temperature cycling of a 1.2 T isothermal remanence applied along the sample [100] (hard) axis.* ***(a)*** *Magnetization vs. temperature and symbols as in Fig. 3* ***(b)*** *Equal-area diagram showing directional change as the sample crosses the Verwey transition. At T > 115 K, directions are slightly steeper and slightly more northerly. At T < 115 K, directions have rotated slightly to the southeast. At T = 115 K, intermediate directions are observed.*

Similar to the [111] case, the total moment decreases on cooling across the Verwey transition followed by an abrupt rebound at 115 K. However, in this case, a clear – if slight – directional change accompanies the rebound (Fig. 4). This can be seen both in the stereo plot (Fig. 4b) and in the relative axis-to-axis variability in magnetization changes across the transition (Fig. 4a).

These two simple test cases clearly demonstrate the potential of the instrument. If one were restricted to single-axis measurements, such subtle directional changes would be extremely difficult to deduce. We hope that this test data set will get both senior and student researchers excited about designing their own experiments.

Community Access

The instrument is still in the development phase, but will ultimately be available to the community through visits to the IRM. If you have a specific application in mind, we encourage you to contact us so that we can keep it in mind as the final engineering and software development stages are completed.

References

Özdemir, Ö., and D. Dunlop, Low-temperature properties of a single crystal of magnetite oriented along principal magnetic axes, *Earth Planet. Sci. Lett.*, 165, 229-239, 1999.

University of Minnesota
291 Shepherd Laboratories
100 Union Street S. E.
Minneapolis, MN 55455-0128
phone: (612) 624-5274
fax: (612) 625-7502
e-mail: irm@umn.edu
www.irm.umn.edu

Nonprofit Org.
U.S Postage
PAID
Mpls., MN
Permit No. 155

The IRM Quarterly

The *Institute for Rock Magnetism* is dedicated to providing state-of-the-art facilities and technical expertise free of charge to any interested researcher who applies and is accepted as a Visiting Fellow. Short proposals are accepted semi-annually in spring and fall for work to be done in a 10-day period during the following half year. Shorter, less formal visits are arranged on an individual basis through the Facilities Manager.

The *IRM* staff consists of **Subir Banerjee**, Professor/Founding Director; **Bruce Moskowitz**, Professor/Director; **Joshua Feinberg**, Assistant Professor/Associate Director; **Jim Marvin**, Emeritus Scientist; **Mike Jackson**, **Peat Sølheid**, and **Julie Bowles**, Staff Scientists.

Funding for the *IRM* is provided by the **National Science Foundation**, the **W. M. Keck Foundation**, and the **University of Minnesota**.

The *IRM Quarterly* is published four times a year by the staff of the *IRM*. If you or someone you know would like to be on our mailing list, if you have something you would like to contribute (*e.g.*, titles plus abstracts of papers in press), or if you have any suggestions to improve the newsletter, please notify the editor:

Julie Bowles
Institute for Rock Magnetism
University of Minnesota
291 Shepherd Laboratories
100 Union Street S. E.
Minneapolis, MN 55455-0128
phone: (612) 624-5274
fax: (612) 625-7502
e-mail: jbowles@umn.edu
www.irm.umn.edu

UNIVERSITY OF MINNESOTA

REGISTER NOW:

The Eighth Santa Fe Conference on Rock Magnetism

June 24 - 27, 2010
St. Johns College
Santa Fe, New Mexico

More information on pg. 2
(or www.irm.umn.edu/SantaFe8/)